22. B. Fiedler, R. M. Mantel, *Doc. Math.* **5**, 695 (2000).
23. J. P. Keener, J. J. Tyson, *Science* **239**, 1284 (1988).
24. A. S. Mikhailov, *Foundations of Synergetics I. Distributed Active Systems* (Springer, Berlin, ed. 2, 1995).
25. A. Yu. Abramychev, V. A. Davydov, A. S. Mikhailov, *Biophysics* **35**, 520 (1990).
26. S. Alonso, F. Sagués, A. S. Mikhailov, in preparation.
27. The higher perturbation terms, responsible for renormalization of the filament tension coefficient, have been computed under an assumption that the amplitude of breathing of a ring filament is small as compared with its radius. Because the amplitude of breathing diverges in the limit $\Delta\omega \rightarrow 0$, this imposes a restriction near the resonance at $\Delta\omega = 0$.
28. I. Aranson, I. Mitkov, *Phys. Rev. E* **58**, 4556 (1998).
29. The authors acknowledge financial support from the REACTOR program of the European Science Foundation and from Dirección General de Investigación (Spain) under project BXX2000-0638-C02. S.A. was financially supported by a grant from the Ministerio de Ciencia y Tecnología (Spain).

6 November 2002; accepted 16 January 2003
Published online 30 January 2003;
10.1126/science.1080207
Include this information when citing this paper.

Recent Trends in Arctic Surface, Cloud, and Radiation Properties from Space

Xuanji Wang[1]* and Jeffrey R. Key[2]

Trends in satellite-derived cloud and surface properties for 1982 to 1999 show that the Arctic has warmed and become cloudier in spring and summer but has cooled and become less cloudy in winter. The increase in spring cloud amount radiatively balances changes in surface temperature and albedo, but during summer, fall, and winter, cloud forcing has tended toward increased cooling. This implies that, if seasonal cloud amounts were not changing, surface warming would be even greater than that observed. Strong correlations with the Arctic Oscillation indicate that the rise in surface temperature and changes in cloud amount are related to large-scale circulation rather than to local processes.

Recent studies have shown that Northern Hemisphere sea-ice extent and thickness have been decreasing (*1*, *2*), whereas land surface air temperature has increased markedly over the past 30 years (*3*). Arctic climate change has also been noted in the horizontal flux of precipitable water (PW), snowfall, and vegetation (*4*–*6*). Although these studies generally agree that the Arctic has been warming, it is not clear how other aspects of the climate system have responded. Have cloud characteristics changed? How do changes in surface and cloud properties interact with and affect the surface radiation budget; i.e., what is the cloud-radiation feedback?

Data from the Advanced Very High Resolution Radiometer (AVHRR) Polar Pathfinder (APP) project (*7*) for the period 1982 to 1999 are used to estimate surface, cloud, and radiation properties. The daily data are centered on a local solar time of 14:00 (high sun) and subsampled to 25-km pixels. We have extended the standard APP product (hereafter APP-x) to include all-sky surface temperature and broadband albedo, cloud properties (amount, particle phase, effective radius, optical depth, temperature, and pressure), radiative fluxes, and the cloud radiative effect, or cloud "forcing." Processing was done as described in (*8*), with atmospheric profile data from the National Center for Environmental Prediction–National Center for Atmospheric Research (NCEP/NCAR) reanalysis (*9*) and ozone from the International Satellite Cloud Climatology Project (ISCCP) D2 data set (*10*). The extended products have been validated with data collected during Arctic field experiments and with data from Arctic and Antarctic meteorological stations (*11*–*14*).

Trend analysis of cloud, surface, and radiation parameters was performed with linear least-squares fit regression. Unless noted otherwise, all trends reported here are significant at the 90% confidence level or higher. Figure 1 shows seasonal and annual trends of surface temperature and surface albedo data over land and ocean north of 60°N. The surface temperature has decreased at the decadal rate of −0.34°C in winter (December through February) but at a confidence level of only 69%. For the area north of 80°N (not shown), the APP-x surface temperature has decreased at −2.2°C per decade. The wintertime sur-

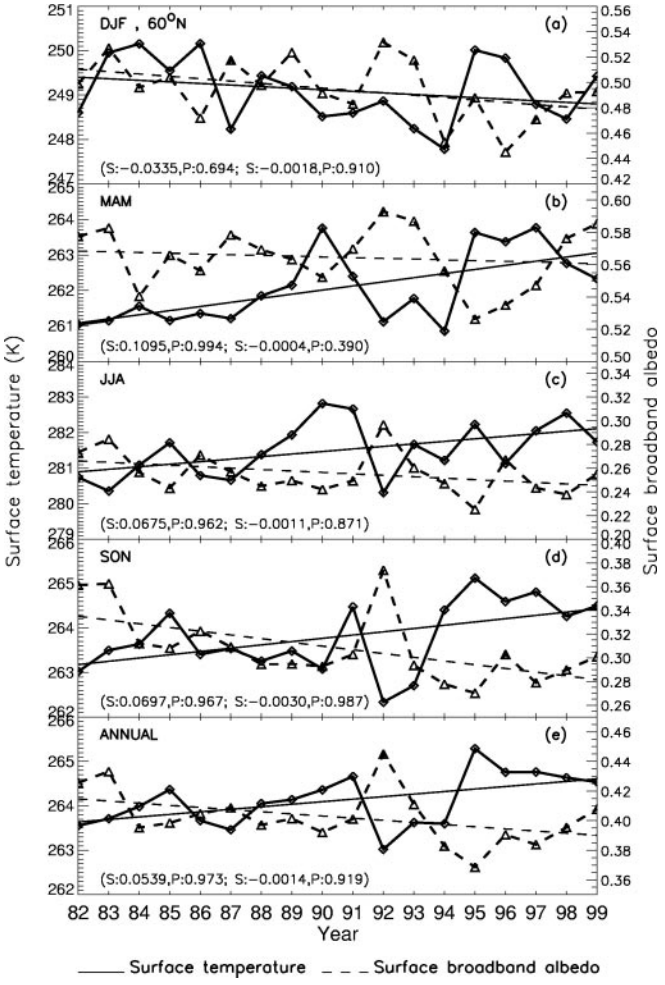

Fig. 1. Time series and trends of surface skin temperature and broadband albedo in winter [December, January, February (DJF)], spring [March, April, May (MAM)], summer [June, July, August (JJA)], and autumn [September, October, November (SON)], and the annual mean during the period 1982 to 1999 for the Arctic north of 60°N. The numbers in parentheses are the trend slope per year (S) and the F test confidence level (P). The first pair of S and P values denotes the surface temperature trend (solid line), and the second pair is for the surface albedo (dashed line).

[1]Cooperative Institute for Meteorological Satellite Studies, University of Wisconsin–Madison, 1225 West Dayton Street, Madison, WI 53706, USA. [2]Office of Research and Applications, National Oceanic and Atmospheric Administration, National Environmental Satellite, Data, and Information Service, 1225 West Dayton Street, Madison, WI 53706, USA.

*To whom correspondence should be addressed. E-mail: xuanjiw@ssec.wisc.edu

face albedo of sunlit areas (60°N to 76°N) has decreased –1.8% per year. Figure 2 shows a cooling trend in winter in the central and eastern Arctic Ocean. During spring, summer, and autumn, the surface temperature has increased over the Arctic at the decadal rates of 1.1, 0.68, and 0.7°C, respectively. The surface albedo has decreased at the decadal rate of −3.0% in autumn, indicating a longer melt season and a later onset of freeze-up and snowfall. On an annual time scale, surface temperature has increased at a rate of 0.54°C per decade. The surface albedo has decreased at the decadal rate of −1.4%.

These results are consistent with surface air-temperature data from 41 Arctic meteorological stations that show winter cooling in the eastern Arctic over the past 20 years (*14*, *15*), with an increasing trend in Arctic winter sea-ice extent (*3*), and with satellite-derived surface temperature and PW (*4*). Albedo trends are consistent with decreases in sea-ice extent, estimated with satellite passive microwave radiometers (*1*).

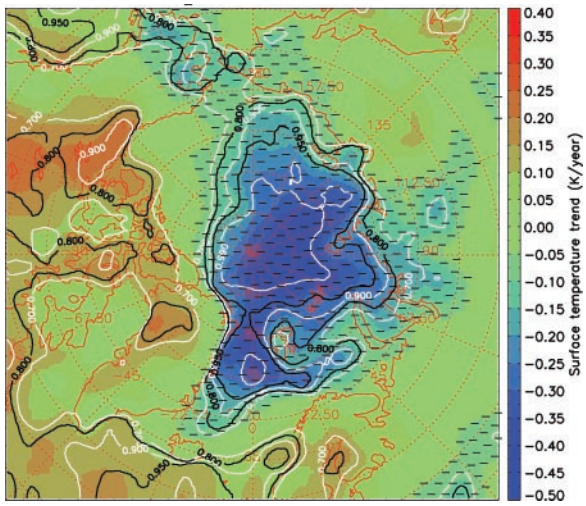

Fig. 2. Surface skin temperature trends over the Arctic in winter, 1982 to 1999. Greenland is in the lower left portion of the image, Alaska is at the upper left, and the North Pole is at the center. The colors represent the trend in kelvin per year. Contours give the statistical level of confidence of the trend. Areas with cooling trends are marked with dashes.

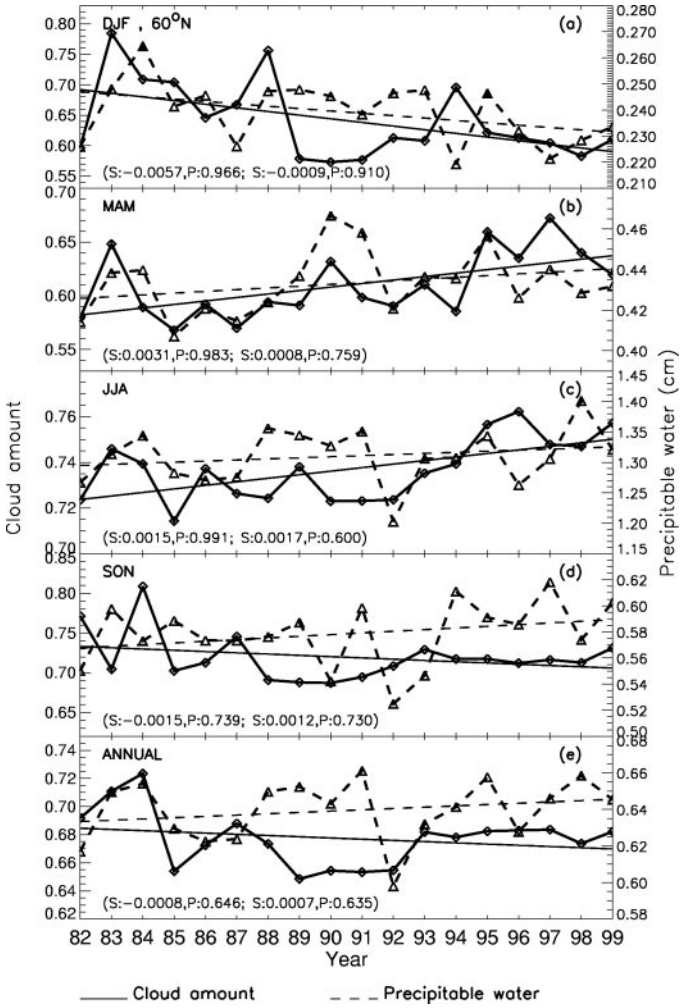

Fig. 3. As in Fig. 1, but for the cloud amount (solid line) and precipitable water (dashed line) trends. The first pair of S and P values denotes the cloud amount trend (solid line), and the second pair denotes the PW trend (dashed line).

Some cloud characteristics have also changed. Figure 3 gives the seasonal and annual trends of satellite-derived cloud amount and PW from the NCEP reanalysis. The winter cloud amount has decreased at the decadal rate of −0.057 (unitless on a scale of 0 to 1) with the largest decrease in the central Arctic Ocean. Spring and summer cloud amount has been increasing at the decadal rates of 0.031 and 0.015, respectively. The increase in cloud amount is generally consistent with an increasing trend in cyclonic activity (*3*) and an increasing trend in total PW. On an annual time scale, the seasonal trends cancel. Over the ocean (not shown) there is a strong decreasing trend in PW during winter at the decadal rate of −0.01 cm, while during spring and autumn PW has been increasing at the decadal rates of 0.013 cm and 0.020 cm, respectively.

Cloud particle effective radius, defined as the ratio of the third to second moments of the particle size distribution, has been decreasing at the decadal rates of −2.5, −0.8, and −1.5 μm for spring, summer, and autumn, respectively. This decrease indicates a greater frequency of liquid-phase cloud in the warmer troposphere, which agrees with reported tropospheric warming trends (*16*). There is no statistically significant trend in cloud optical depth over the study period. There are significant trends in cloud height only for the autumn and winter over the western Arctic Ocean, where cloud pressure has decreased somewhat. If the increasing cloud amount were due to increasing surface evaporation, as might be expected with surface warming, low cloud amount would probably increase as well. This does not appear to be the case.

The cloud radiative effect, or cloud forcing, is defined as the difference between the net all-sky flux and the net clear-sky flux, so that a positive cloud forcing indicates a warming effect and a negative value indicates a cooling effect. Changes in cloud forcing reflect changes in surface temperature, surface albedo, and cloud properties. The wintertime net cloud forcing, which is primarily longwave forcing, has decreased at a decadal rate of −4.50 W/m^2 (decreasing warming effect) in response to the decreasing cloud amount and surface temperature (Fig. 4). In spring, increasing cloud amount results in a strong increase in the longwave cloud forcing (greater warming) but a decrease in the shortwave cloud forcing (greater cooling), so that the net effect is near zero. During summer the

large solar flux, increasing cloud amount, and decreasing albedo result in a trend toward increasing cloud cooling by −5.17 W/m^2 per decade. There is also an increasing cloud cooling trend in the fall, largely a result of decreasing albedo, because there is only a weak trend in cloud amount. The annual trend in net cloud forcing is −3.17 W/m^2, indicating an increasing cooling effect.

These trends imply that the cooling effect of clouds may be damping the increase in surface temperature to some degree, i.e., if cloud amount were not increasing during spring and summer, then the surface temperature might be increasing at an even greater rate. It appears that during the sunlit portion of a year, the decreases in sea ice extent and albedo that result from surface warming modulate the increasing cloud cooling effect, resulting in little or no change in the surface radiation budget.

The extent to which the significance of the trends is affected by calibration and algorithm uncertainties is discussed in detail elsewhere (*14*, *17*) but is summarized here. An examination of the intercalibration between satellites in the 18-year record reveals no observable bias or inconsistency. A probability analysis addressing the likelihood of obtaining trends by chance was done with two sets of uncertainties reported in the literature. The probability of finding a trend in a sample from a population with no trend is negligible for the set of smaller calibration uncertainties. For the set of larger uncertainties it is possible, but not probable, that artificial trends could be found for surface temperature and albedo, but not for cloud amount or surface net cloud forcing. However, given that our surface-temperature trends generally agree in sign and magnitude with surface measurements across the Arctic, and that albedo trends are consistent with those reported in the literature for related parameters, it is improbable that our trends are an artifact of calibration uncertainty.

Remote sensing of polar clouds is inherently difficult as a result of ubiquitous temperature inversions, bright surfaces, low temperatures, low sun angles, and long polar nights. As such, high-latitude retrieval algorithm uncertainties are generally larger than are those for other geographic areas. However, systematic biases will have no impact on trends, and algorithm uncertainties for area- and time-averaged data, as is the case here, will be smaller than the magnitude of the trends, even if uncertainties for instantaneous observations are relatively large. If biases are not consistent over time, then trends will be affected. Unfortunately, the scarcity of validation data does not allow us to assess the consistency of algorithm biases, with one exception. A comparison of the APP-x all-sky surface temperature to the surface air-temperature measurements from 41 Arctic meteorological stations (*15*) shows that the two surface temperature data sets are consistently within 1 to 3 K of each other throughout the 1982 to 1999 period, and that the trends are similar in magnitude and sign. Because the satellite retrievals of cloud and radiative fluxes are closely related to the retrieval of surface temperature and albedo, we can have confidence in those trends as well.

Are these changes due to large-scale advective processes rather than to local radiative effects? The correlation between surface temperature and the Arctic Oscillation (AO) index (*18*), which can be used to represent large-scale circulation patterns, is shown in Fig. 5. The correlations are as expected: positive in northern Europe and northern Russia but negative over Greenland and northern Canada. Given the increasing cooling effect of clouds found here, the rise in surface temperature is clearly related to large-scale circulation. The decreasing albedo is a response to a warming Arctic, with less sea ice, earlier melt, and later freeze-up. At present, however, it is unclear to what extent changes in cloud characteristics are due to local processes (e.g., evaporation) or to large-scale circulation.

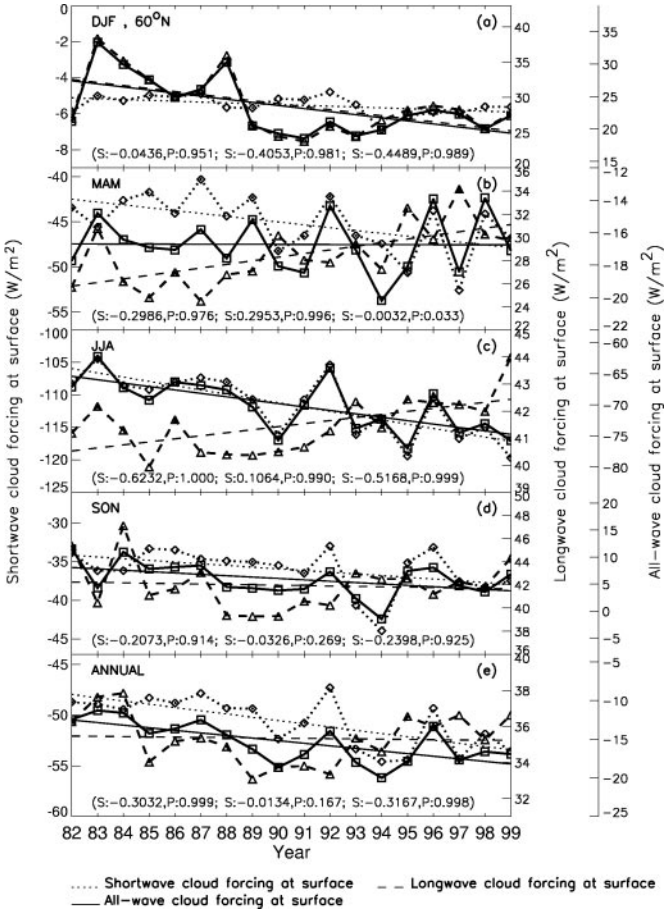

Fig. 4. As in Fig. 1, but for the surface shortwave cloud forcing (dotted line), longwave cloud forcing (dashed line), and net all-wave cloud forcing (solid line) trends. The first pair of S and P values denotes the surface shortwave cloud forcing trend (dotted line), the second pair denotes the longwave cloud forcing trend (dashed line), and the last pair denotes the net all-wave cloud forcing trend (solid line).

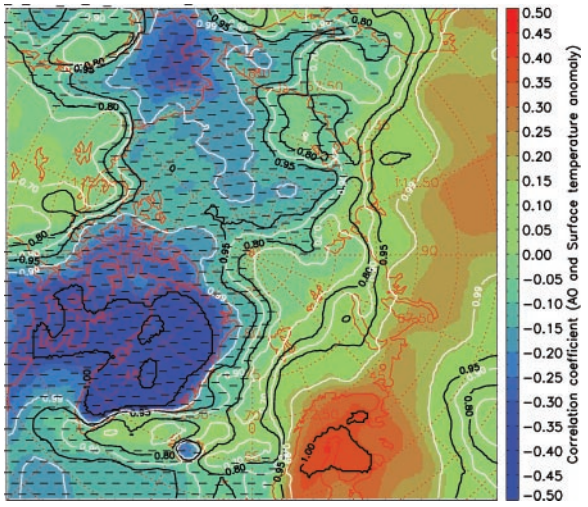

Fig. 5. Correlation coefficient image between the monthly AO index and the surface-temperature anomaly during the period 1982 to 1999. The geographic coverage is the same as in Fig. 2. The color scale indicates the correlation coefficient value; the contours give the confidence levels based on Student's *t* test. Areas with negative correlations are marked with dashes.

References and Notes

1. C. L. Parkinson, D. J. Cavalieri, P. Gloersen, H. J. Zwally, J. C. Comiso. *J. Geophys. Res.* **104**, 20837 (1999).
2. K. Y. Vinnikov *et al.*, *Science* **286**, 1934 (1999).
3. M. C. Serreze *et al.*, *Clim. Change* **46**, 159 (2000).
4. D. G. Groves, J. A. Francis, *J. Geophys. Res.* **107**, 10.1029/2002JD002285 (2002).
5. W. L. Chapman, J. E. Walsh, *Bull. Am. Meteorol. Soc.* **74**, 33 (1993).
6. R. B. Myneni, C. D. Keeling, C. J. Tucker, G. Asrar, R. R. Nemani, *Nature* **386**, 698 (1997).
7. W. Meier, J. A. Maslanik, J. R. Key, C. W. Fowler, *Earth Interactions* **1** (no. 5), 1) (1997); available online at http://earthinteractions.org.
8. J. Key, "The cloud and surface parameter retrieval (CASPR) system for polar AVHRR" (Cooperative Institute for Meteorological Satellite Studies, University of Wisconsin, Madison, 2002). Available at http://stratus.ssec.wisc.edu/caspr/.
9. R. Kistler *et al.*, *Bull. Am. Meteorol. Soc.* **82**, 247 (2001).
10. W. B. Rossow, A. Walker, D. Beuschel, M. Roiter, "International Satellite Cloud Climatology Project (ISCCP) Documentation of Cloud Data" (World Climate Research Programme, NASA, Goddard Institute of Space Studies, 1996).
11. J. R. Key, X. Wang, J. Stroeve, C. Fowler, *J. Geophys. Res.* **106**, 12489 (2001).
12. J. A. Maslanik, J. R. Key, C. W. Fowler, T. Nguyen, X. Wang, *J. Geophys. Res.* **106**, 15233 (2001).
13. J. Stroeve, J. Box, C. Fowler, T. Haran, J. Key, *Remote Sens. Environ.*, **75**, 360 (2001).
14. For details on algorithm uncertainties, see Supporting Text 1.
15. I. V. Polyakov *et al.*, *J. Clim.*, in press (2002). Data are available at www.frontier.iarc.uaf.edu/~igor/data/airtemppres.php.
16. J. E. Overland, W. Muyin, N. A. Bond, *J. Clim.* **15**, 1702 (2002).
17. For a discussion of calibration uncertainties, see Supporting Text 2.
18. D. W. J. Thompson, J. M. Wallace, *Geophys. Res. Lett.* **25**, 1297 (1998).

19. Supported by the National Oceanic and Atmospheric Administration and the National Science Foundation. We thank C. Fowler, J. Maslanik, T. Scambos, and T. Haran for their work on the AVHRR Polar Pathfinder data set.

Supporting Online Material

www.sciencemag.org/cgi/content/full/299/5613/1725/DC1
Supporting Text 1
Figs. S1 to S11
Table S1
References
Supporting Text 2
Figs. S1 to S10
Tables S1 and S2
References

4 September 2002; accepted 10 February 2003

Timing of Atmospheric CO_2 and Antarctic Temperature Changes Across Termination III

Nicolas Caillon,[1,2]* Jeffrey P. Severinghaus,[2] Jean Jouzel,[1] Jean-Marc Barnola,[3] Jiancheng Kang,[4] Volodya Y. Lipenkov[5]

The analysis of air bubbles from ice cores has yielded a precise record of atmospheric greenhouse gas concentrations, but the timing of changes in these gases with respect to temperature is not accurately known because of uncertainty in the gas age–ice age difference. We have measured the isotopic composition of argon in air bubbles in the Vostok core during Termination III (~240,000 years before the present). This record most likely reflects the temperature and accumulation change, although the mechanism remains unclear. The sequence of events during Termination III suggests that the CO_2 increase lagged Antarctic deglacial warming by 800 ± 200 years and preceded the Northern Hemisphere deglaciation.

Ice cores are unique archives of past climatic and environmental conditions that provide detailed records of local temperature and atmospheric concentrations of greenhouse gases. Analyses of the Vostok ice core in Antarctica (*1*) show that concentrations of carbon dioxide correlate well with Antarctic temperature throughout the last four climatic cycles, with glacial-interglacial CO_2 increases of 80 to 100 parts per million by volume (ppmv) (*1–4*). Determining the mechanisms that cause these variations is important for understanding climate change, but the explanation for the strong link between atmospheric CO_2 and Antarctic air temperature is still unclear (*5*). One reason for this uncertainty is that the relative timing of temperature and CO_2 changes is not accurately known (*6*). The temporal relation between these two quantities is difficult to discern because air is trapped in ice at the base of the firn layer (*7*), where, at low accumulation sites such as Vostok, ice may be 6000 years old. The gas age–ice age difference (Δage) may be uncertain by 1000 years or more (*1*) and thus obscures the phasing of gas variations with climate signals borne by the ice. Although Δage and the associated uncertainty are lower at other sites where CO_2 deglacial records are available (*8*, *9*), we do not yet have a clear answer about the timing of CO_2 and Antarctic temperature changes during Terminations.

One way to circumvent this difficulty is to use records of atmospheric CO_2 content and temperature contained only in the trapped gases. During firnification, air composition is slightly modified by physical processes such as gravitational and thermal fractionation. As a result of this latter process, detectable anomalies in nitrogen and argon isotopic composition ($\delta^{15}N$ and $\delta^{40}Ar$) develop during episodes of rapid climatic changes such as those recorded in Greenland ice cores (*10–14*). Even though we expected that thermal anomalies would be hardly detectable in the Vostok core (*15*), we searched with $\delta^{40}Ar$ measurements for a thermal signal at the start of a Termination. Given the quality and the availability of the Vostok ice, we focused first on Termination III, dated at 240,000 years before present. We observed a $\delta^{40}Ar$ change across this Termination that is closely correlated with the deuterium temperature record (*16*). This change appears to result mostly from gravitational fractionation in response to a change in the diffusive column height (DCH) (*17*), although recent model results suggest that it can be partly due to thermal fractionation (*18*). Although we do not yet clearly understand the underlying mechanisms, we argue that the $\delta^{40}Ar$ record can be taken as a climate proxy, thus providing constraints about the timing of CO_2 and climate change during Termination III.

All $\delta^{40}Ar$ measurements have been performed at the Scripps Institution of Oceanography following a wet extraction method (*19*) and using ice from the more recent 5Γ Vostok core. A new detailed deuterium record with a resolution of 20 years or less has been measured (Fig. 1). It is in excellent agreement with published data (*1*) confirming, in particular, a two-step warming somewhat similar to what is observed for Termination I, with a return to colder conditions in the first part of the Termination. The $\delta^{40}Ar$ record (Fig. 1A) shows an increase of ~0.25‰ from 2815 to 2775 m (which occurs in two steps with a return to relatively low values around 2800 m). Such a $\delta^{40}Ar$ increase is indicative of an augmentation of the DCH by 11 m [or ~6 m if the part potentially resulting from thermal diffusion (*18*, *19*) is subtracted]. This result is surprising because firn densification models (*20*) predict that total firn thickness decreases in this depth interval. Similarly, the $\delta^{40}Ar$ decrease observed from 2775 to 2740 m corresponds to a depth interval over which the modeled total firn thickness increases (Figs. 1B and 2).

[1]Institut Pierre Simon Laplace/Laboratoire des Sciences du Climat et de l'Environnement, Commissariat à l'Energie Atomique/CNRS, L'Orme des Merisiers, CEA Saclay, 91191, Gif sur Yvette, France. [2]Scripps Institution of Oceanography, University of California San Diego, La Jolla, CA 92093–0244, USA. [3]Laboratoire de Glaciologie et Géophysique de l'Environnement, CNRS, BP96, 38402, Saint Martin d'Hères, France. [4]Polar Research Institute of China, Pudong, Shanghai, 200129, People's Republic of China. [5]Arctic and Antarctic Research Institute, Beringa Street 38, 199397 St. Petersburg, Russia.

*To whom correspondence should be addressed. E-mail: ncaillon@ucsd.edu